IEEE Access
Multidisciplinary | Rapid Review | Open Access Journal

Received May 6, 2019, accepted May 29, 2019, date of publication June 6, 2019, date of current version June 20, 2019.

Digital Object Identifier 10.1109/ACCESS.2019.2921316

Optimal Allocation of Hybrid Energy Storage Systems for Smoothing Photovoltaic Power Fluctuations Considering the Active Power Curtailment of Photovoltaic

WEI MA[1], (Student Member, IEEE), WEI WANG[1], XUEZHI WU[1], RUONAN HU[1], (Student Member, IEEE), FEN TANG[1], WEIGE ZHANG[1], XIAOYAN HAN[2], AND LIJIE DING[2]

[1]National Active Distribution Network Technology Research Center, Beijing Jiaotong University, Beijing 100044, China
[2]State Grid Sichuan Electric Power Company, Chengdu 610041, China

Corresponding author: Wei Ma (16117385@ bjtu.edu.cn)

This work was supported by the National Key Research and Development Program of China under Grant 2018YFB0905200.

ABSTRACT Hybrid energy storage systems (HESSs) have become an effective solution for smoothing the active power variations of photovoltaic (PV). In order to reduce the required capacities and costs of the HESS, a coordinated control scheme is developed to mitigate the power variations of a PV plant by using the HESS and the active power curtailment (APC) of PV. Furthermore, a multi-objective optimization model is established to dispatch the output power of batteries and supercapacitors, considering the overall losses and the state-of-charge (SOC) deviation of the supercapacitor. Based on the proposed smoothing strategy, an allocation model is developed to optimize the energy and power capacities of the HESS with the aim of maximizing the annual net income of the PV and HESS plant. The numerous simulations are carried out to verify the effectiveness of the proposed smoothing and allocation methods by using the real data of a PV plant. In addition, we also discuss the impacts of the different dispatching strategies of the HESS, grid requirements of power variations, and solution methods on the HESS allocation results.

INDEX TERMS Hybrid energy storage system (HESS), photovoltaic (PV) power fluctuation, capacity allocation, active power curtailment.

I. INTRODUCTION

To cope with the problems of climate change and environmental pollution, the penetration of renewable energy (e.g., wind and solar energy) in power systems has gradually increased in recent years [1]. However, the active power variations of large-scale PV plants can cause voltage fluctuations of power supply systems, resulting in a decline in power quality [2], [3]. Nevertheless, they may seriously threaten the reliability and stability of the utility grids if increasing the penetration of PV in the future [4]. Therefore, the power variations of grid-connected PV plants should be mitigated within a specific range, such as $1\% \sim 5\%$/min of its installed capacity proposed by Mexico [5] and 10%/min proposed by the Puerto Rico Electric Power Authority (PREPA) [3].

In recent years, using battery energy storage (BES) has become a popular way to smooth active power variations of grid-connected PV plants at the point of common coupling (PCC) [5]–[9]. A 16MW/71MWh BES system was built in the Zhangbei national demonstration project of China, where the upward (downward) active power variations are smoothed by charging (discharging) BES [6]. Furthermore, several control strategies of BES were developed to achieve better results of smoothing PV power variations and reducing the costs of batteries [5], [10]–[12].

To overcome the shortages of BES, such as lower cycle life, lower efficiencies, and lower power rates [13]–[15], the hybrid energy storage system (HESS) is a better solution to smooth power variations of PV because it combines the

The associate editor coordinating the review of this manuscript and approving it for publication was Shantha Jayasinghe.

advantages of batteries and supercapacitors [16]. The supercapacitor energy storage (SCES) can provide higher power rates during a short time, and its cycle life is extremely long [17]. However, its cost per kWh is quite expensive. Hence it is unacceptable to install too many supercapacitors in a HESS [13], [14]. Consequently, a practical allocation method of the HESS is needed to find its optimal energy and power capacities, in order to achieve lower costs of a PV plant and better performances of smoothing power variations.

Several works have been done on optimizing the locations and capacities of BES systems in active distribution networks or microgrids [12], [18]–[21]. They are aimed at preventing voltage violations caused by the uncertainty of demand and renewable energy [19], minimizing the total costs considering correlated forecast uncertainties of dispatchable resources [21]. Also, the sizing problems of the BES have been investigated with the aim of peak shaving and optimal power flow of power systems [18].

However, there is relatively little published research on the optimal allocation of the HESS [18], [22]–[24]. A techno-economic model is established to optimize the capacities of a HESS by minimizing the net present cost of systems, where the HESS is used to smooth power fluctuations of a PV plant [23]. Concerning the peak shaving of power systems, the spectral analysis method is utilized to solve the allocation problem of the HESS under a higher penetration level of wind power [22]. Also, to reduce the power shortage rate of loads and line losses in active distribution networks, the HESS capacities are optimized considering the demand side response [24].

To the best of our knowledge, the sizing problem of a HESS has still not been extensively examined when using the HESS and the active power curtailment (APC) of PV to smooth PV power variations [25], [26]. The main idea of the APC is to reduce the active power of PV converters when needed, instead of keeping them always operating in the maximum point of power tracking (MPPT) mode [10]–[12], [25]. The APC of PV can reduce the required capacities of a HESS. Thus its corresponding investment and operating costs can be reduced. On the other hand, the APC of PV may cause an energy reduction in PV generation [12], [25]. As a result, the trade-off between them needs further discussions.

In summary, this paper focuses on the optimal HESS sizing method when using the HESS and the APC of PV to smooth the active power variations of a grid-connected PV plant. The main contributions of this work are summarized as follows:

(1) A coordinated smoothing strategy is developed to mitigate the power variations at the PCC by coordinating the HESS output power and the power reduction in the PV.

(2) A multi-objective optimization model of the HESS is established to assign the total compensation power of the HESS to the BES and the SCES with the aim of (a) minimizing the total losses of the HESS, and (b) optimizing the state of charge (SOC) of the SCES.

(3) Based on the proposed smoothing strategy, an allocation model is developed to optimize the energy and power capacities of the HESS, which fully considers the power variation requirements of PV, energy losses caused by the APC of PV, system investment costs, and the cycle aging costs of batteries. Furthermore, to ensure the feasibility of optimization results, numerous scenarios of the PV power variations are considered in this allocation model.

(4) The proposed smoothing strategy and the allocation model are conducted on the actual active power data of a 750kW PV plant. Numerous simulations are carried out to verify the effectiveness and correctness of them. Moreover, we have discussed the impacts of the PV power variation requirements, initial parameters of the dispatching strategy of the HESS, and the solution methods on the optimal allocation results of the HESS.

The rest of the paper is organized as follows: Section II describes the system structure of a PV plant with a HESS. The mathematical model of the proposed smoothing strategy is presented in Section III, including the overall control scheme of the HESS and PV for smoothing power variations and the optimization model of dispatching the HESS power. Section IV discusses the optimal allocation model of the HESS. Case studies and discussions are presented in Section V, and the conclusions of this work are summarized in Section VI.

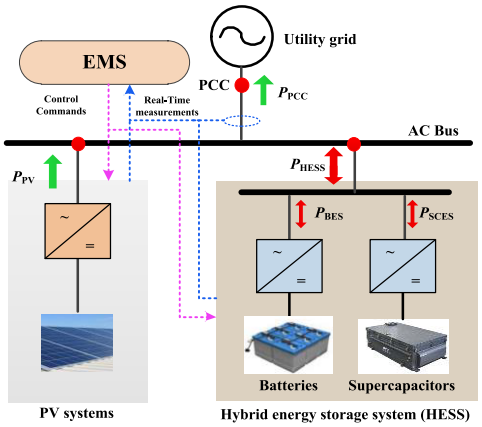

FIGURE 1. System topology and information flows of a PV plant including a HESS.

II. SYSTEM DESCRIPTION

Fig. 1 presents the system topology of a PV plant including a HESS, which is used to mitigate the variations of the active power injected into the utility from PV systems by charging or discharging. The HESS consists of the BES and the SCES, which are connected to the same AC bus. The overall power of the HESS denoted by P_{HESS} is the sum of the BES power, P_{BES}, and the SCES power, P_{SCES}. The active power of PV is denoted by P_{PV}.

The energy management system (EMS) can receive real-time data of the PV systems, the BES, and the SCES every 5 seconds. At the same time, the EMS will update their power commands calculated by the proposed smoothing strategies,

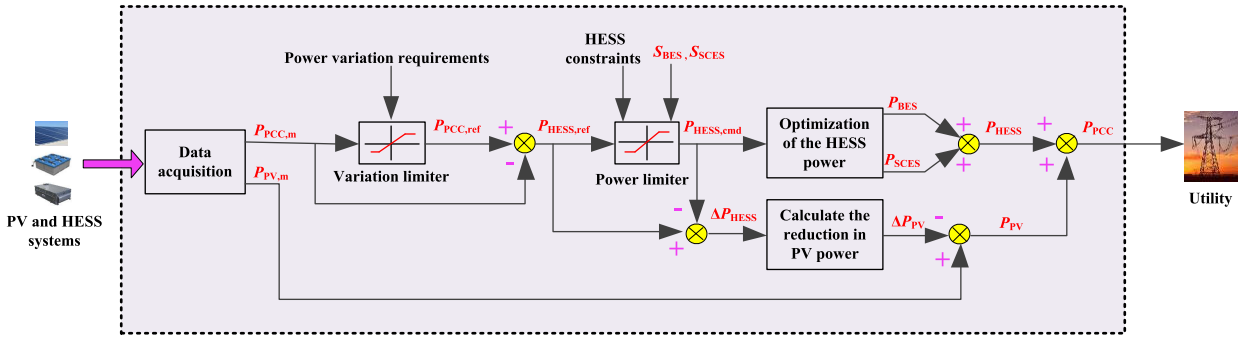

FIGURE 2. Control methods of the PV and the HESS for smoothing PV power fluctuations.

ensuring the power variations at the PCC can meet the predetermined requirements.

In addition, this paper mainly focuses on the variations of active power generated by PV plants, thus neglecting the impacts of the variations of reactive power.

III. SMOOTHING STRATEGY

In this section, the active power variations of a PV plant at the PCC is defined in *subsection A*. Then, the basic idea of the proposed smoothing strategy is briefly described in *subsection B,* and the detailed control methods of the HESS and the PV converter are discussed in *subsection C*. Finally, the optimal power dispatching strategy of the HESS is presented in *subsection D*.

A. DEFINITION OF THE ACTIVE POWER VARIATIONS OF A PV PLANT

This study mainly investigates the power variation of PV in a time scale of one minute. Therefore, we define that the power variation at time t is the difference between the maximum and minimum active power injected into the utility within 1min. The details of this definition are explained as follows.

Before the HESS provides the compensation power at time t, the power generated by PV is denoted by $P_{\mathrm{PV,\,m}}(t)$, and $P_{\mathrm{PCC,\,m}}(t)$ denotes the power measured at the PCC. Note that $P_{\mathrm{PV,\,m}}(t)$ is equal to $P_{\mathrm{PCC,\,m}}(t)$ because the HESS has not provided any compensation power at this moment. Let $\delta(t)$ denote a set of the active power values measured at the PCC from time t_0 to t, thus $\delta(t) = \{P_{\mathrm{PCC}}(t_0), P_{\mathrm{PCC}}(t_0 + \Delta t), \ldots, P_{\mathrm{PCC}}(t - \Delta t), P_{\mathrm{PCC,\,m}}(t)\}, t \in \{5:00, 5:00 + \Delta t, 5:00 + 2\Delta t, \ldots, 20:00\}, t_0 = t - -1$ min, $\Delta t = 5$s is the sampling interval.

Overall, before the suppression, the current power variation, $\Delta P_{\mathrm{PCC}}(t)$, can be calculated as follows:

$$\Delta P_{\mathrm{PCC}}(t) = \begin{cases} P_{\max} - P_{\min}, & \text{if } t_2 \text{ is earlier than } t_1. \\ P_{\min} - P_{\max}, & \text{otherwise.} \end{cases} \quad (1)$$

where $P_{\max}$ denotes the largest element of the set $\delta(t)$, and t_1 denotes the moment when $P_{\max}$ appears, while $P_{\min}$ denotes the smallest element of the set $\delta(t)$, and t_2 denotes the moment when $P_{\min}$ appears.

This study requires that the variation of the PV power at the PCC should less than $\pm 10\% C_{PV}$/min [3], where C_{PV} is the installed capacity of a PV plant. Namely, if $|\Delta P_{PCC}(t)| > 10\% C_{PV}$, smoothing methods are required to absorb the excessive power variations.

B. BASIC RULES OF THE PROPOSED SMOOTHING STRATEGY

This paper uses the HESS and the APC of PV to jointly smooth power variations of PV, and the general ideas of the proposed smoothing strategy are as follows.

The PV power fluctuations can be divided into two types: (a) downward fluctuations, and (b) upward fluctuations. The downward fluctuations are smoothed by discharging the HESS, while the upward fluctuations are smoothed by charging the HESS and reducing the output power of PV. Namely:

(1) If the upward power fluctuation exceeds the maximum allowable charging power of the HESS, considering its SOC and power capacity constraints, the excessive power fluctuation will be absorbed by reducing the PV power. At the same time, the HESS will be charged with the maximum allowable power. Otherwise, the upward power fluctuation will be completely smoothed by the HESS, and let the PV operate in the MPPT mode.

(2) On the other hand, smoothing downward power fluctuations only relies on the HESS because the APC of PV cannot help to smooth them by limiting the outputs of PV.

C. CONTROL METHODS OF THE HESS AND THE PV CONVERTER

According to the basic rules discussed above, Fig. 2 shows the specific control methods of the PV converter and the HESS for smoothing power variations at the PCC.

As can be seen from Fig. 2, according to the power variation requirements, the variation limiter outputs the reference power of the PCC, $P_{\mathrm{PCC,\,ref}}(t)$, as follows:

$$P_{\mathrm{PCC,ref}}(t) = \begin{cases} P_{\min} + P_{\mathrm{var,max}}, & \text{if } \Delta P_{\mathrm{PCC}}(t) > P_{\mathrm{var,max}} \\ P_{\max} - P_{\mathrm{var,max}}, & \text{if } \Delta P_{\mathrm{PCC}}(t) < -P_{\mathrm{var,max}} \\ P_{\mathrm{PCC,m}}(t), & \text{otherwise.} \end{cases} \quad (2)$$

where the values of $P_{\max}$ and $P_{\min}$ are directly gained from (1); $P_{\text{var, max}}$ is the upper limit of the PV power variation, and $P_{\text{var, max}} = 10\%C_{PV}$. Hence, the expected compensation power of the HESS, $P_{\text{HESS, ref}}(t)$, is presented in (3).

$$P_{\text{HESS,ref}}(t) = P_{\text{PCC,ref}}(t) - P_{\text{PCC,m}}(t) \tag{3}$$

where $P_{\text{HESS, ref}} > 0$ means that the HESS needs to be discharged. By contrast, $P_{\text{HESS, ref}} < 0$ means that it needs to be charged.

However, the HESS may not adequately supply the required power ($P_{\text{HESS, ref}}(t)$) due to its constraints of SOC and power capacities. Thus its reference power needs to be modified by the power limiter.

In this study, the SOC constraints of batteries and supercapacitors are 20% – 90% and 10% – 90%, respectively. The energy and power capacities of the BES and the SCES are denoted by $C_{\text{E, b}}$, $C_{\text{P, b}}$, $C_{\text{E, sc}}$, and $C_{\text{P, sc}}$, respectively. The real-time SOC data of batteries and supercapacitors are $S_{\text{BES}}(t)$ and $S_{\text{SCES}}(t)$, respectively. Consequently, the maximum available charging and discharging power of the HESS at time t can be gained according to the above constraints and SOC data. They are denoted by $P_{\text{HESS, max}}(t)$ and $P_{\text{HESS, min}}(t)$, respectively, where $P_{\text{HESS, max}} \geq 0$ and $P_{\text{HESS, min}} \leq 0$.

As a result, the real compensation power provided by the HESS is $P_{\text{HESS, cmd}}(t)(|P_{\text{HESS, cmd}}| \leq |P_{\text{HESS, ref}}|)$, as shown in (4).

$$P_{\text{HESS,cmd}}(t) = \begin{cases} P_{\text{HESS,max}}(t), & \text{if} P_{\text{HESS,ref}}(t) > P_{\text{HESS,max}}(t) \\ P_{\text{HESS,min}}(t), & \text{if} P_{\text{HESS,ref}}(t) < P_{\text{HESS,min}}(t) \\ P_{\text{HESS,ref}}(t), & \text{otherwise.} \end{cases} \tag{4}$$

Considering the characteristics of different types of energy storage (BES and SCES), such as efficiencies, cycle lifetime, and power rates, an optimization method is required to dispatch the power between the BES and the SCES, i.e., to ensure that $P_{\text{BES}}(t) + P_{\text{SCES}}(t) = P_{\text{HESS, cmd}}(t)$. Therefore, this paper develops an optimal dispatching strategy of the HESS to address the above concerns, which is discussed in the following section.

Having determined the outputs of the HESS, we need to determine whether or not to reduce the PV power. Unfortunately, reducing PV power only helps to mitigate upward power fluctuations. Therefore, the following three situations are considered:

(1) If the excessive compensation power, $\Delta P_{\text{HESS}}(t)$, which is equal to $P_{\text{HESS, ref}}(t)$ - $P_{\text{HESS, cmd}}(t)$, is less than zero, the PV will actively reduce its output power, ensuring the variation of the power at the PCC can meet the requirements.

(2) If $\Delta P_{\text{HESS}} = 0$, indicating that the HESS has enough capacities to cope with those power variations, the PV does not need to reduce its output power. Hence, it continues to run in the MPPT mode.

(3) If $\Delta P_{\text{HESS}} > 0$, the HESS will be discharged with the maximum allowable power, while keeping the PV running in the MPPT mode. In order to ensure the HESS can completely mitigate those downward variations, it is necessary to allocate its capacities reasonably and control the SOC of batteries and supercapacitors properly, which are discussed below.

In summary, the final output power of the PV converter is calculated by (5).

$$P_{\text{PV}}(t) = \begin{cases} P_{\text{PV,m}}(t) - \Delta P_{\text{PV}}(t), & \text{if } \Delta P_{\text{HESS}}(t) < 0 \\ P_{\text{PV,m}}(t), & \text{otherwise.} \end{cases} \tag{5}$$

where $\Delta P_{PV}(t)$ is the power reduction in PV converters, and $\Delta P_{PV}(t) = -\Delta P_{\text{HESS}}(t)$.

Consequently, through the coordination between the HESS and the APC of PV, the variations of the active power at the PCC are entirely within the allowable range.

D. OPTIMAL POWER DISPATCHING STRATEGY OF THE HESS

This section discusses how to optimize the HESS power when its overall power command, $P_{\text{HESS, cmd}}(t)$, has been determined by (4). Hence, a multi-objective optimization model for the HESS is developed to dispatch the outputs of the BES and the SCES, where the decision variables are $P_{\text{BES}}(t)$ and $P_{\text{SCES}}(t)$. The objective functions and constraints of this model are explained as follows.

1) OBJECTIVE FUNCTION

There are two objectives considered in the established optimization model:

(1) To reduce total energy losses of the HESS and prolong the actual service life of the BES, the SCES is preferred to provide more compensation power because its overall efficiency (90% - 95% [27]) is larger than that of the BES (80% - 90% [27]). Moreover, the number of cycles of the lithium-ion battery is quite small, about one-tenth of that of a supercapacitor [27]. To this end, the sub-objective function f_1 is described as follows:

$$\min f_1 = \left[\mu_1 \left|P_{\text{BES}}(t)\right| + \mu_2 \left|P_{\text{SCES}}(t)\right|\right] \Delta t \tag{6}$$

where μ_1 and μ_2 are the loss factors of the BES and SCES, respectively. In this work, $\mu_1 = 10\%$, $\mu_2 = 5\%$ [27].

(2) The SCES needs to reserve some energy to smooth the sudden rise or drop in the PV power. Thus the reference value of its SOC is set to 50%. To this end, the sub-objective function f_2 is applied to minimize the deviation of the SCES SOC, as follows:

$$\min f_2 = \frac{\left|S_{\text{SCES}}(t - \Delta t) - P_{\text{SCES}}(t)\Delta t / C_{\text{E,sc}} - 50\%\right|}{\Delta S_{\text{SCES,max}}} \tag{7}$$

where $\Delta S_{\text{SCES, max}}$ is the maximum possible SOC deviation of the SCES, and $\Delta S_{\text{SCES, max}} = 40\%$ because its SOC constraint is [10%, 90%].

2) MULTI-OBJECTIVE OPTIMIZATION MODEL

Combining the two sub-objective functions (f_1 and f_2), a multi-objective optimization model is established in (8),

where $\beta(0 \le \beta \le 1)$ is the weight coefficient and its value is discussed in the following section.

Objective function:

$$\min f(P_{\mathrm{BES}}, P_{\mathrm{SCES}}) = \beta \frac{f_1 - f_{1,\min}}{f_{1,\max} - f_{1,\min}} + (1-\beta) f_2 \quad (8)$$

In (8), the range of f_1 is $[f_{1,\min}, f_{1,\max}]$, which is used for normalization. The normalization of f_2 is not required because its range is [0, 1].

Constraints:

$$P_{\mathrm{BES}}(t) + P_{\mathrm{SCES}}(t) = P_{\mathrm{HESS,cmd}}(t) \quad (9)$$

$$P_{\mathrm{BES}}(t) \times P_{\mathrm{SCES}}(t) \ge 0 \quad (10)$$

$$\begin{cases} |P_{\mathrm{BES}}(t)| \le C_{\mathrm{P,b}} \\ |P_{\mathrm{SCES}}(t)| \le C_{\mathrm{P,sc}} \end{cases} \quad (11)$$

$$\begin{cases} 20\% \le S_{\mathrm{BES}}(t-\Delta t) - \dfrac{P_{\mathrm{BES}}(t)\Delta t}{C_{\mathrm{E,b}}} \le 90\% \\ 10\% \le S_{\mathrm{SCES}}(t-\Delta t) - \dfrac{P_{\mathrm{SCES}}(t)\Delta t}{C_{\mathrm{E,sc}}} \le 90\% \end{cases} \quad (12)$$

where (9) is the power balance constraint; (10) requires that the power flow directions of the BES and the SCES should not be opposite at time of t; (11) is the power capacity constraint, and (12) is the SOC constraint.

3) ADAPTIVE CONTROL METHOD FOR WEIGHT COEFFICIENT

In this study, the weight coefficient, β, is not a constant, while it varies with the real-time state of the supercapacitor's SOC. Hence an adaptive control method is proposed to dynamically adjust the value of β.

In a HESS, compared with the BES, the energy capacity of the SCES is usually allocated much smaller due to its higher capital costs, but its power capacity is usually larger because supercapacitors can be charged or discharged with higher power rates [14]. When there is a sharp drop in PV power, the HESS needs to be discharged continuously for a while, because its total discharging power and time are determined by the magnitude and the requirement of PV power variations. However, if β is a constant, the supercapacitor's SOC will quickly reach its lower limit, which may significantly weaken the smoothing ability of the HESS.

Therefore, this study only adjusts the value of β when the HESS is discharging; otherwise, β is a predefined constant because the APC of PV can help to smooth the upward power variations if the supercapacitor's SOC reaches its upper limit, as follows:

$$\beta(t) = \begin{cases} g(S_{\mathrm{SCES}}(t-\Delta t)), & \text{if } P_{\mathrm{HESS,cmd}}(t) > 0 \\ \beta_0, & \text{otherwise.} \end{cases} \quad (13)$$

where g(x) is a piecewise function, as shown in (14) and Fig. 3; β_0 is the initial weight coefficient determined by the analytic hierarchy process (AHP) method [28]. In this work, $\beta_0 = 0.7$.

$$g(x) = \begin{cases} 0, & \text{if } 0 \le x \le 10\% \\ k(x+b)^3, & \text{if } 10\% < x < 50\% \\ \beta_0, & \text{otherwise.} \end{cases} \quad (14)$$

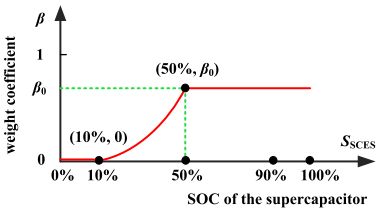

FIGURE 3. Schematic diagram of the piecewise function g(x).

where k and b are related to β_0 and the SOC constraint of the SCES. In this work, $b = -0.1$ and $k = \beta_0/(0.5+b)^3$.

IV. OPTIMAL ALLOCATION MODEL OF THE HESS

This section establishes an allocation model to optimize the energy and power capacities of the HESS when the smoothing strategy discussed above is utilized to smooth the power variations of a PV plant.

A. PROBLEM DESCRIPTION

The decision variables of this problem are $C_{\mathrm{E,b}}$, $C_{\mathrm{P,b}}$, $C_{\mathrm{E,sc}}$, and $C_{\mathrm{P,sc}}$. For a PV plant, the capacity optimization results of the HESS should achieve the following two aims:

(1) The optimal energy and power capacities of the HESS can cope with the various power variations of this PV plant.

(2) The net income of this PV plant should be the largest with the optimal solution.

In addition to the above concerns, it is vital to consider the charging and discharging characteristics of supercapacitors and batteries, such as C-rates and cycle lifetime, instead of only maximizing the system revenues. Also, the energy losses caused by the APC of PV and the initial investment costs of systems need to be carefully considered.

Furthermore, to reduce the total calculation time, it is reasonable to evaluate the annual revenues and costs of the HESS and PV systems by using several typical days of PV data rather than the whole year data.

B. MATHEMATICAL MODEL

A nonlinear programming optimization model is established to maximize the annual net income of the PV plant while optimizing the HESS capacities. The objective function, ζ, consists of the following five parts:

(a) The PV plant can benefit from providing solar energy to utilities, and its annual revenue is denoted by R_{sell}.

(b) The initial investment costs of systems are converted into the equivalent annual investment costs denoted by O_{inv}.

(c) The annual operation and maintenance costs of systems are denoted by O_{OM}.

(d) The cycle aging costs of batteries, $O_{\mathrm{c,b}}$, are considered due to its limited lifetime (about 2000-5000 full cycles), while the cycle aging costs of supercapacitors are neglected because its lifetime is even more than 500000 full cycles [27].

(e) A penalty function, C_{pf}, is added in this model to assess the performance of smoothing power variations of PV. i.e., if the variations of the smoothed PV power are acceptable, then C_{pf} is equal to zero; otherwise, the value of C_{pf} is quite large.

Objective function:

$$\max \zeta\ (\mathbf{d}) = \left(R_{\text{sell}} - O_{\text{inv}} - O_{\text{OM}} - O_{\text{c,b}}\right) - C_{\text{pf}} \quad (15)$$

where $\mathbf{d}$ is the decision variable, and $\mathbf{d} = [C_{\text{E, b}}, C_{\text{P, b}}, C_{\text{E, sc}}, C_{\text{P, sc}}]$. The details of the function R_{sell}, O_{inv}, O_{OM}, $O_{\text{c, b}}$, and C_{pf} are explained in the following section.

Constraints:

$$0 < C_{\text{P,b}}, C_{\text{P,sc}} \leq C_{\text{PV}} \quad (16a)$$

$$0 < C_{\text{E,b}} \leq C_{\text{E,b,max}} \quad (16b)$$

$$0 < C_{\text{E,sc}} \leq C_{\text{E,sc,max}} \quad (16c)$$

$$C_{\text{P,b}}/C_{\text{E,b}} \leq \delta_1 \quad (16d)$$

$$C_{\text{P,sc}}/C_{\text{E,sc}} \geq \delta_2 \quad (16e)$$

In (16), (16a) indicates that the power capacities of HESS should be less than the PV capacity. $C_{\text{E, b,max}}$ and $C_{\text{E, sc, max}}$ are upper limits of the energy capacities of the BES and the SCES, respectively. Considering the C-rate of a battery, (16d) requires that the power and energy ratio of the BES should be less than δ_1 ($\delta_1 > 0$). Considering the SCES can be charged or discharged with a higher C-rate, its power and energy ratio should be greater than $\delta_2(\delta_2 > 0)$. In addition, in this work, $\delta_1 = 1$, $\delta_2 = 10$ [22]–[24].

C. CALCULATION METHODS OF THE OBJECTIVE FUNCTION

In the following, $\mathbf{T}$ is a set of all the sampling points in a day, $\mathbf{T} = \{t_1, t_2, \ldots, t_n\}$, and $t_j \in \mathbf{T}$, $1 \leq j \leq n$. Let set $\mathbf{D}$denote the typical days of PV power variations, $\mathbf{D} = \{d_1, d_2, \ldots, d_m\}$, and $d_i \in \mathbf{D}$, $1 \leq i \leq m$. Also, the probabilities corresponding to each typical day are denoted by a set $\mathbf{P} = \{p_1, p_2, \ldots, p_m\}$, and $p_i \in \mathbf{P}$. For example, $P_{\text{BES}}(t_j, d_i)$ is the active power of the BES at time t_j on the d_i^{th} day; p_m represents the probability of the typical day d_m in a year.

1) ANNUAL REVENUE OF SELLING PV POWER (R_{sell})

The annual revenue of selling PV power is presented in (17), where ρ_{elec} is the unit price of solar power (\$/kWh).

$$R_{\text{sell}} = 365\rho_{\text{elec}}\Delta t \sum_{\substack{d_i \in \mathbf{D} \\ p_i \in \mathbf{P}}} p_i \left(\sum_{t_j \in \mathbf{T}} P_{\text{PCC}}(t_j, d_i)\right) \quad (17)$$

2) ANNUAL INVESTMENT COSTS OF SYSTEMS (O_{inv})

The initial investment costs of the PV, the BES, and the SCES are denoted by I_1, I_2, and I_3, respectively. They are as follows:

$$I_1 = \rho_{\text{pv}} C_{\text{PV}} \quad (18a)$$

$$I_2 = \rho_{\text{bat}} C_{\text{E,b}} + \rho_{\text{pcs}} C_{\text{P,b}} \quad (18b)$$

$$I_3 = \rho_{\text{sc}} C_{\text{E,sc}} + \rho_{\text{pcs}} C_{\text{P,sc}} \quad (18c)$$

where ρ_{pv}, ρ_{bat}, ρ_{sc}, and ρ_{pcs} are the capital costs related to the capacities of the PV plant, batteries, supercapacitors, and converters, respectively (\$/kWp, \$/kWh, \$/kWh, and \$/kW).

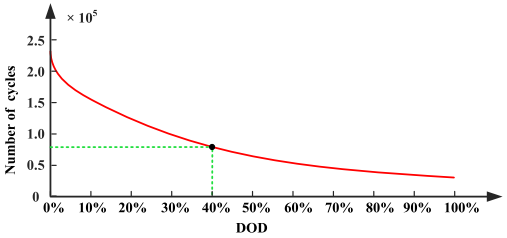

FIGURE 4. The number of cycles of a lithium-ion battery at various DODs.

The initial investment costs of them are converted into the annual investment costs related to their lifetime L_1, L_2, and L_3 (years).

$$O_{\text{inv}} = \sum_{k=1}^{3} I_k \frac{r(1+r)^{L_k}}{(1+r)^{L_k} - 1} \quad (19)$$

where r is the discount rate, and $r = 10\%$ [29].

3) ANNUAL OPERATION AND MAINTENANCE COSTS OF SYSTEMS (O_{OM})

O_{OM} is related to the operating losses of the HESS and the fixed maintenance costs of systems, as shown follows:

$$O_{\text{OM}} = r_1 I_1 + r_2 (I_2 + I_3) + 365\rho_{\text{elec}}\Delta t \times \sum_{\substack{d_i \in \mathbf{D} \\ p_i \in \mathbf{P}}} p_i \left(\sum_{t_j \in \mathbf{T}} \mu_1 \left|P_{\text{BES}}(t_j, d_i)\right| + \mu_2 \left|P_{\text{SCES}}(t_j, d_i)\right|\right) \quad (20)$$

where r_1 and r_2 are coefficients used to calculate the fixed maintenance costs, and $r_1 = 0.2\%$, $r_2 = 0.5\%$ [25].

4) ANNUAL CYCLE AGING COSTS OF BATTERIES ($O_{c, b}$)

The degradation of lithium-ion batteries is a complicated electrochemical process affected by several factors, such as depth of discharge (DOD), temperatures, and C-rates [30]. In order to simplify the analysis, this study only takes into account the impacts of various DODs on the battery's degradation. The relationships between the number of cycles of a battery, N_{bat}, and DODs, d_{fc}, are described in (21) and shown in Fig. 4 [31].

$$N(d_{\text{fc}}) = N_{\text{cycle,100\%}}\ (d_{\text{fc}})^{-k_{\text{p}}} \quad (21)$$

where $N_{\text{cycle,100\%}}$ is the number of cycles if $d_{\text{fc}} = 100\%$; k_p is a constant, $0.8 \leq k_{\text{p}} \leq 2.1$, which can be determined by a curve fitting method according to the battery's datasheets [31]. In addition, $N_{\text{cycle,100\%}} = 2500$ and $k_{\text{p}} = 1.759$ in this work [32].

However, it is hard to ensure that every two adjacent charging and discharging processes can form a full cycle with a specific DOD. Therefore, the rainflow counting algorithm (RCA) [32], [33] is utilized to count the equivalent full cycles of the BES, as shown in Fig. 5.

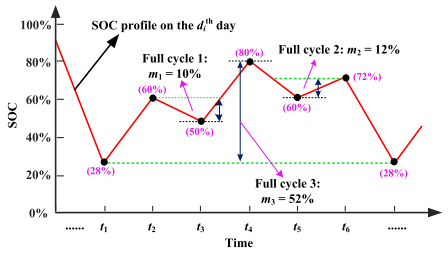

FIGURE 5. A schematic diagram of counting the equivalent full cycles of batteries by using the RCA.

As can be seen from Fig. 5, when providing a SOC profile of the BES on the d_i^{th} day, $d_i \in \mathbf{D}$, the RCA can output the total number of full cycles, $N_{\text{full}}(d_i)$, and the DODs of each full cycle, $d_{\text{fc}}(h, d_i)$, $h = 1, 2, \ldots, N_{\text{full}}(d_i)$.

In conclusion, the battery cycle aging costs can be evaluated by a function related to the DOD of each full cycle and the initial investment costs of the battery, as described follows:

$$O_{\text{cycle}} = 365 \sum_{\substack{d_i \in \mathbf{D} \\ p_i \in \mathbf{P}}} p_i \left(\sum_{h=1}^{N_{\text{full}}(d_i)} \frac{\rho_{\text{bat}} C_{\text{E,b}}}{N_{\text{cycle,100\%}}} d_{\text{fc}}(h, d_i)^{k_{\text{p}}} \right) \tag{22}$$

5) PENALTY FUNCTION (C_{pf})

The penalty function,C_{pf}, is described in (23), where a is a pretty large constant; $E_{\text{exceed}}^{\text{now}}$ and $E_{\text{exceed}}^{\text{ago}}$ represent the amounts of the power variations that are larger than ±10%/min before and after smoothing, respectively. The range of C_{pf} is [0, a], and $a = 10^8$ in this work. Also, $0 \le E_{\text{exceed}}^{\text{now}} \le E_{\text{exceed}}^{\text{ago}}$.

$$C_{\text{pf}} = \alpha \left(E_{\text{exceed}}^{\text{now}} / E_{\text{exceed}}^{\text{ago}} \right) \tag{23}$$

where $E_{\text{exceed}}^{\text{ago}}$ can be calculated by (24), and the same formulas can be used to calculated $E_{\text{exceed}}^{\text{now}}$ if $\Delta P_{\text{PCC}}(t_j)$ represents the power variations at the PCC after the suppression.

$$P_{\text{excess}}(t_j) = \begin{cases} \left|\Delta P_{\text{PCC}}(t_j)\right| - P_{\text{var,max}}, \\ \qquad \text{if } \left|\Delta P_{\text{PCC}}(t_j)\right| > P_{\text{var,max}} \\ 0, \\ \qquad \text{otherwise.} \end{cases} \tag{24a}$$

$$E_{\text{exceed}}^{\text{ago}} = 365 \Delta t \sum_{\substack{d_i \in \mathbf{D} \\ p_i \in \mathbf{P}}} p_i \left(\sum_{t_j \in \mathbf{T}} P_{\text{excess}}(t_j, d_i) \right) \tag{24b}$$

D. SOLUTION METHODS

This study uses the particle swarm optimization algorithm with inertia weight (PSO-IW) [34] to solve the optimal allocation model of the HESS because it has been widely used in numerous fields, such as the optimization of active distribution networks, the voltage and frequency regulation, and the optimal power flow [35], [36]. The overall idea of using the PSO-IW to solve the established allocation model is shown in Fig.6, and the specific solution processes are as follows:

Algorithm 1 Optimize the HESS Capacities Using the PSO-IW Algorithm (Upper Level)

1: Input data: power variation requirements, economic parameters, and other necessary parameters.
2: Set parameters of the PSO-IW algorithm: such as population sizes, $N_{\max}$, and the number of iterations, N_{iterate}.
3: Initialize the population: $\mathbf{V}^{(1)} = [\mathbf{d}_1^{(1)}, \mathbf{d}_2^{(1)}, \ldots, \mathbf{d}_{N\max}^{(1)}]$.
4: Start iteration:
5: **for** $k = 1$ **to** N_{iterate} **do**
6: Call the ***smoothing strategy*** and calculate the values of the objective function, $\zeta(\mathbf{V}^{(k)})$.
7: Update the best population, $\mathbf{d}_{\text{best}}$.
8: Generate a new set of populations, $\mathbf{V}^{(k+1)}$.
9: **end for**
10: Output the optimal capacities of the HESS, $\mathbf{d}_{\text{best}}$, and the optimal value of the objective function, $\zeta(\mathbf{d}_{\text{best}})$.

Algorithm 2 Smoothing Strategy (Lower Level)

1: Input data: population, $\mathbf{V}^{(k)}$, the number of the typical days, N_{typd}, active power data of each typical day, etc.
2: **for** $a = 1$ **to** $N_{\max}$ **do**
3: Set the energy and power capacities of the HESS equal to $\mathbf{d}_a^{(k)}$.
4: **for** $b = 1$ **to** N_{typd} **do**
5: The **proposed smoothing strategy** is applied to the typical day b.
6: Save the smoothing results.
7: **end for**
8: Calculate the objective function, $\zeta(\mathbf{d}_a^{(k)})$.
9: **end for**
10: Return the values of the objective function, $\zeta(\mathbf{V}^{(k)})$.

In this work, all optimization models and solution methods are programmed on the MATLAB @R2015b platform. Furthermore, to solve the multi-objective optimization model (8) when dispatching the output power of the BES and the SCES, the optimization tool *fmincon*(·) provided by the MATLAB toolboxes is used, because it can effectively solve this problem with less computing time.

V. CASE STUDY

A. TYPICAL DAYS OF PV POWER VARIATIONS

In this work, the typical days, which can reflect the general characteristics of the PV power variations, were established

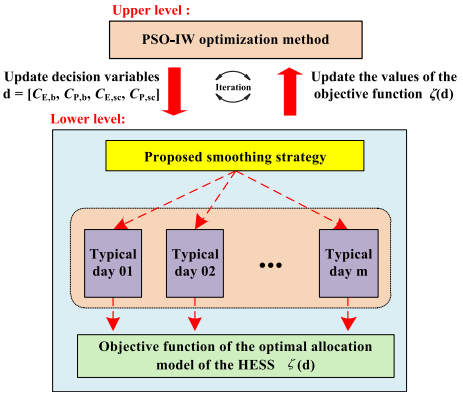

FIGURE 6. Overall idea of using the PSO-IW to solve the established allocation model.

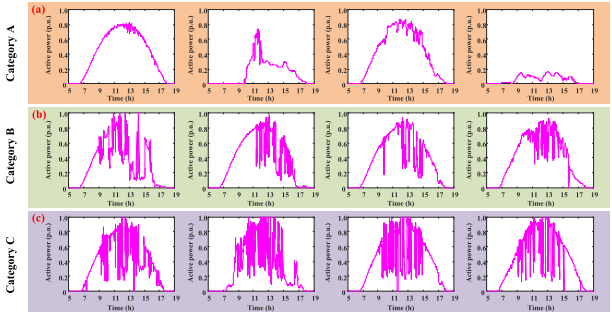

FIGURE 7. Typical days of PV power variations: (a) category A has the lowest level of power variations, including sunny, rainy, and snowy days; (b) category B has the medium level of power variations; and (c) category C has the highest level of power variations, representing the PV power on cloudy days.

based on the real data of a 750kWp PV plant in Sri Lanka. The data recorded the active power of this PV plant from January 01, 2012 to November 31, 2012 (365 days) with the sampling interval of 5s.

These data sets were divided into three main categories by using the K-means clustering algorithm [37], according to the magnitude and frequency of power variations. The number of days included in each category is 55 days (15%), 204 days (56%), and 106 days (29%), respectively. To reduce computing time, four days of data were selected from each category as the typical days of PV power variations (total 12 days), as shown in Fig. 7.

B. SIMULATION PARAMETERS

Simulation parameters are configured as shown in Table 1, where the economic parameters of PV systems, lithium-ion batteries, supercapacitors, and converters are obtained according to the latest IRENA reports [38]–[40]. The price of selling PV power is obtained from the official website of the U.S. Energy Information Administration [41].

C. ALLOCATION RESULTS

Based on the same typical days shown in Fig. 7, the optimal energy and power capacities of the HESS of the two different smoothing strategies, including the proposed strategy and the reference strategy proposed in [26], were calculated using

TABLE 1. Simulation parameters.

Name	Symbol	Value
Capacity of the PV plant	C_{PV}	750 (kWp)
Requirements of power variations	$P_{var,max}$	75 (kW/min)
Capital cost of PV systems	ρ_{pv}	1150 ($/kW)
Capital cost of lithium-ion batteries	ρ_{bat}	570 ($/kWh)
Capital cost of supercapacitors	ρ_{sc}	5800 ($/kWh)
Capital cost of converters	ρ_{pcs}	105 ($/kWh)
Price of solar power	ρ_{elec}	0.13 ($/kWh)
Lifetime of PV systems	L_1	25 (years)
Lifetime of lithium-ion batteries	L_2	8 (years)
Lifetime of supercapacitors	L_3	10 (years)
The number of typical days	N_{typd}	12 (days)
Probabilities of typical days	$p_1 \sim p_4$	3.75%
	$p_5 \sim p_8$	14.0%
	$p_9 \sim p_{12}$	7.25%
Population sizes of the PSO-IW	N_{max}	50
The number of iterations	$N_{iterate}$	200

the established optimal allocation model. Different from the proposed smoothing strategy, the reference strategy only uses the HESS to smooth power variations without limiting the PV power. The allocation results are presented in Table 2.

As can be seen from Table 2, the proposed allocation model is suitable for optimizing the HESS capacities of different smoothing strategies. The energy capacity of the SCES of the reference strategy is significantly larger (about 125%) than that of the proposed strategy, while the other optimal capacities of them are almost the same. They indicate that the APC of PV can help to reduce the supercapacitor's capacity. Thus the corresponding initial investment costs of the SCES can be much smaller. Furthermore, the annual energy losses of the HESS are smaller, resulting from the optimization of dispatching the compensation power of the HESS and the reduced utilization ratio of the HESS due to the APC of PV.

It is clear that the total amount of the annual PV power generation of the proposed smoothing strategy is reduced by about 0.0805% due to the curtailed PV energy, causing the revenue reduction in selling PV energy. However, from the perspective of the comprehensive economics of the PV plant, using the proposed strategy to mitigate the power variations of PV plants can improve its annual net income, reduce the initial investment costs of systems, and reduce the overall capacities and operating losses of the HESS.

D. SMOOTHING RESULTS

To verify the correctness of the optimal allocation results, i.e., $\mathbf{d}_{best} = [180, 170, 24, 390]$, a typical day was selected from category C in Fig. 7 to evaluate the smoothing results of the proposed smoothing strategy. Namely, let the capacities of

TABLE 2. Optimal energy and power capacities of the HESS for two different smoothing strategies.

Results	Proposed smoothing strategy (HESS + APC of PV)	Reference smoothing strategy [26] (only HESS)
Energy capacity of the BES (kWh)	180	175
Power capacity of the BES (kW)	170	162
Energy capacity of the SCES (kWh)	24	30
Power capacity of the SCES (kW)	390	400
Annual energy losses of the HESS (kWh)	9024.33	12126.10
Annual net income ($)	10262.25	5396.91
Annual power generation (kWh)	1305174.3	1306225.5
PV power curtailment loss (% total production)	0.0805%	0.00%

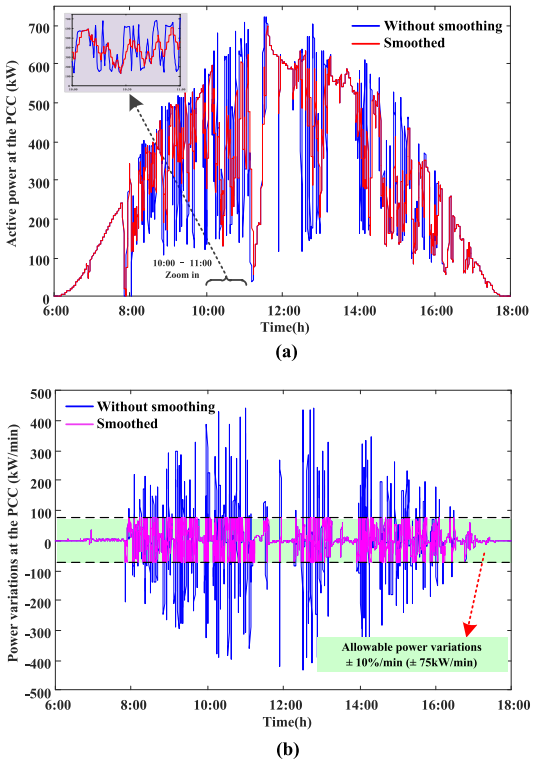

FIGURE 8. Smoothing results of the proposed smoothing strategy: (a) the profiles of the active power at the PCC and (b) power variations at the PCC.

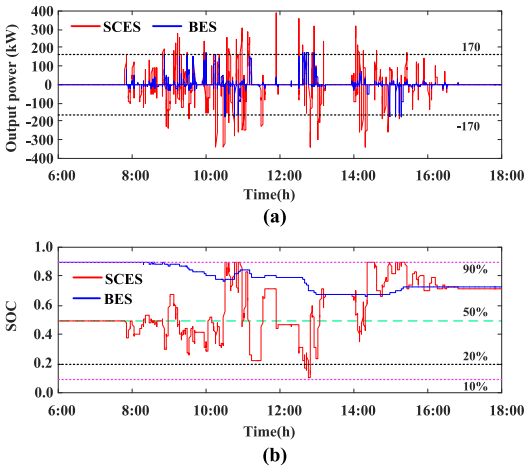

FIGURE 9. Profiles of the active power and SOC of the BES and the SCES: (a) output power and (b) SOC profiles.

the HESS equal to $\mathbf{d}_{\text{best}}$, then the proposed smoothing strategy is used to smooth the power variations of the selected typical day. As a result, after the compensation, the profiles of the active power at the PCC, P_{PCC}, and its variations, ΔP_{PCC}, calculated by (1) are shown in Fig. 8.

It can be clearly seen from the profiles in Fig. 8, the variations of the smoothed PV power are strictly limited to the range of ±10%/min. Furthermore, based on the same capacities of the HESS, i.e., $\mathbf{d}_{\text{best}}$, we also investigated the smoothing results of other several days, which were selected from the category A, B, and C randomly. It was found that the power variations of all those typical days could be effectively suppressed within the allowable range (±10%/min). Therefore, simulation results proved the effectiveness of the proposed smoothing strategy and the correctness of the optimal allocation results.

Fig. 9 shows the profiles of the active power and SOC of the BES and the SCES. In Fig. 9(a), the SCES provided more power components, and its power change rates were faster compared with the BES. In other words, the utilization of the SCES is higher because reducing the overall losses of the HESS is considered in the multi-objective optimization model (sub-objective function f_1 (6)) while dispatching the HESS power. Thus the SCES is preferred. On the other hand, the SOC of the SCES shown in Fig. 9(b) fluctuated within the range of 10% to 90%, and its average value fluctuated around 50%, which was considered in the sub-objective function f_2 (7). They verified the correctness and effectiveness of the established multi-objective optimization model of dispatching the HESS power.

E. DISCUSSIONS

1) INITIAL WEIGHT COEFFICIENT OF THE SMOOTHING STRATEGY

In the proposed smoothing strategy, as shown in Fig. 3, the weight coefficient β of two sub-objective functions (f_1 and f_2) changes with the real-time status of the supercapacitor's SOC, and its initial value was set to 0.7, i.e., $\beta_0 = 0.7$.

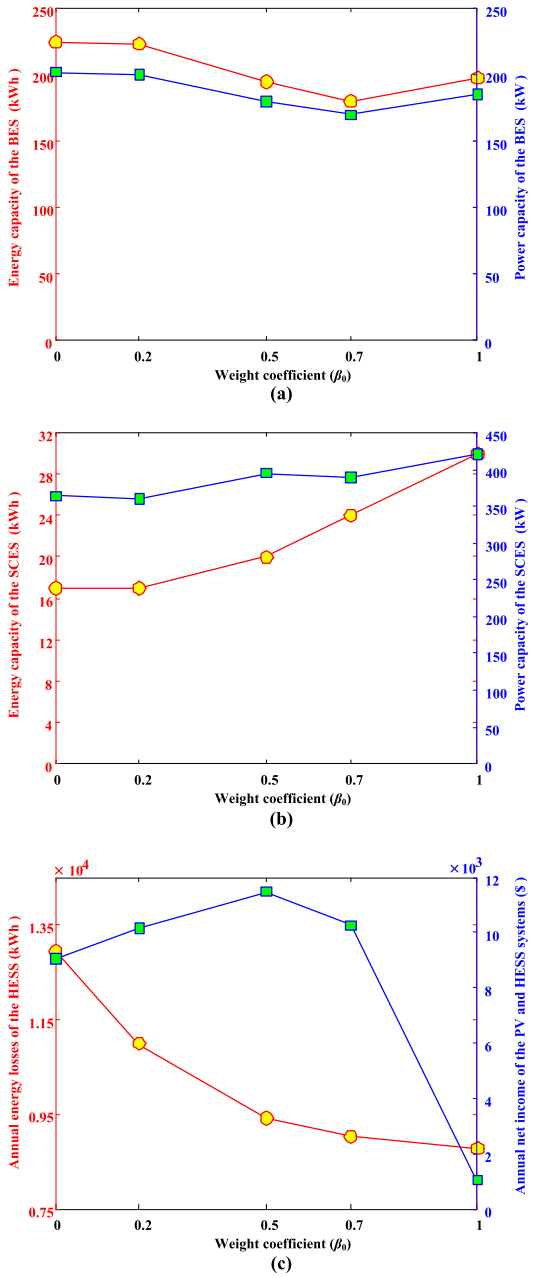

FIGURE 10. Impacts of the initial weight coefficient β_0) of the proposed smoothing strategy on the allocation results of the HESS: (a) optimal BES capacities, (b) optimal SCES capacities, and (c) annual energy losses of the HESS and annual net income of systems with different β_0.

Thus the impacts of the value of β_0 on the allocation results of the HESS need to be discussed. Fig. 10 shows the profiles of the optimal capacities of the BES and the SCES, the total annual losses of the HESS, and the annual net income of systems with the different values of β_0.

Fig. 10(a) shows that there has been a slow decrease in the optimal capacities of the BES when increasing the β_0 from 0 to 0.7, whereas the optimal capacities of the SCES increase steadily (Fig. 10(b)). Nevertheless, it can be seen from Fig. 10(c) that there has been a significant decline in the total energy losses of the HESS, which indicates that β_0 plays an essential role in allocating the HESS capacities because β_0 represents the utilization rate of the SCES while dispatching the power demand of the HESS. The larger the value of β_0, the higher the utilization rate of the SCES. For example, if $\beta_0 = 0$, the SCES is less preferred to respond to the HESS power demand for smoothing PV power variations, thus the optimal capacities of the BES are the largest, and the optimal capacities of the SCES are the lowest. Furthermore, the annual energy losses of the HESS are the highest due to the lower efficiency of the BES, if we set $\beta_0 = 0$.

Another important finding is that the annual net income of systems reaches a peak at $\beta_0 = 0.5$ (as shown in Fig. 10(c)), indicating the system revenue exists a maximum point as β_0 changes. Therefore, based on the simulation results, it is recommended to set the value of β_0 within the range of [0.4, 0.7], achieving the maximum revenue of systems and the reasonable allocation results of the HESS.

2) ALLOWABLE RANGES OF PV POWER VARIATIONS

In this work, the allowable variation range of the PV power was assumed to be ±10%/min. However, when increasing or decreasing the allowable range, the optimal capacities of the BES and the SCES, the energy losses caused by reducing the PV power, and the annual net income of systems are shown in Fig. 11.

The most interesting finding is that there has been a steady decrease in the optimal energy capacity of the SCES when decreasing the allowable range from ±20%/min to ±2%/min (Fig. 11(b)), whereas the optimal energy and power capacities of the BES increase steadily (Fig. 11(a)). This result may be explained by the fact that reducing the allowable variation range results in the HESS needs to absorb more excessive power variations, i.e., the total throughput energy of the HESS is dramatically increased. As a result, the required capacities of the BES need to be increased because the battery is capable of absorbing or releasing sustained energy, while the supercapacitor is good at providing higher rates of power. Furthermore, to maximize the system revenue, the energy capacity of the SCES needs to be reduced due to its expensive costs.

Another important finding is that the frequency of reducing the PV power is increased if the variation requirement is stricter (from ±20% to ±2%/min), thus correspondingly causing more energy losses, as shown in Fig. 11(c). On the other hand, it indicates that the APC of PV will be more effective and useful for helping the HESS achieve a better smoothing result. By contrast, if the allowable range is larger, for example, ±20%/min, the HESS has enough capacities to cope with all power variations, thus limiting PV power is not needed.

Also, it can be seen from Fig. 11(c) that the annual net income of systems can even become negative if the allowable range is less than ±5%/min because the owner of the PV plant needs to install more energy storage systems. This may reduce the motivation of users to develop PV systems. Therefore, the policy makers of utilities should make more

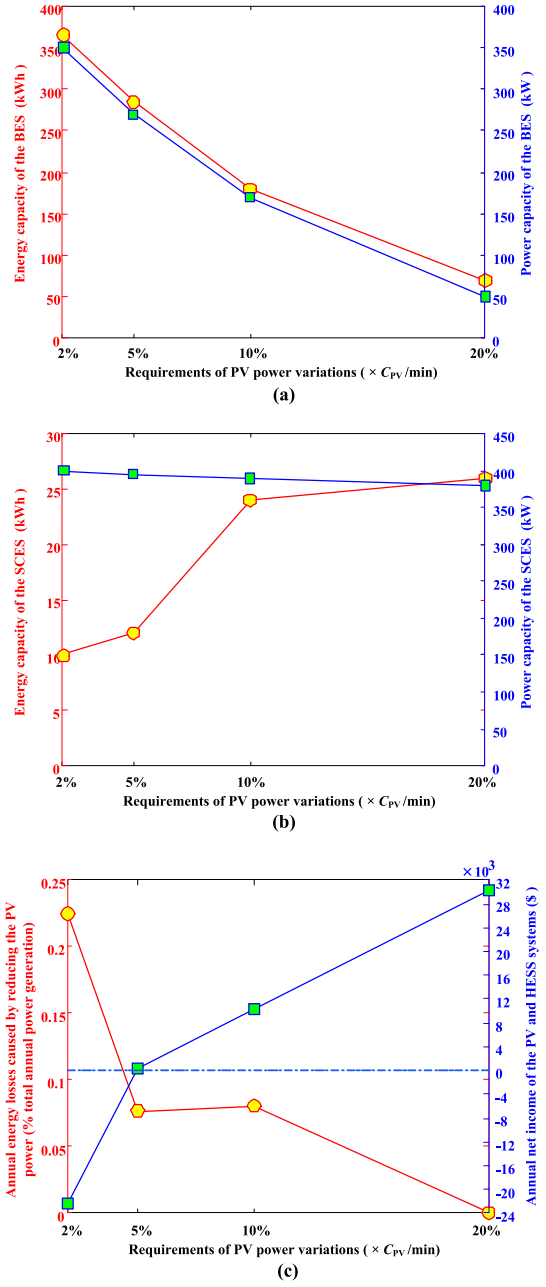

FIGURE 11. Impacts of the power variation requirements on the allocation results of the HESS: (a) optimal BES capacities, (b) optimal SCES capacities, and (c) annual energy losses caused by reducing the PV power and annual net income of systems with different requirements of PV power variations.

contributions to balance the development of renewable energy and the safety and stability of utilities. One possible solution is that the utilities may give some subsidies to owners of PV plants if the power variation requirements are extremely strict.

3) SOLUTION METHODS

This study used the PSO-IW algorithm to optimize the HESS capacities, and the total number of iterations was set to 200. Simulations were conducted on a 64-bit workstation with

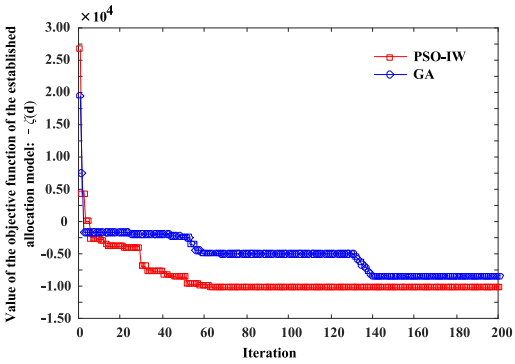

FIGURE 12. Convergence profiles of the objective function ($-\zeta$ (d)) with different solution methods.

Windows 10 Pro, Intel Xeon E5-2609 @2.4-GHz CPU, 12G RAM, and a MATLAB-R2015b platform. The convergence profiles of the objective function, $-\zeta(\mathbf{d})$, with the PSO-IW algorithm and the genetic algorithm (GA) [42] are presented in Fig. 12, where the total computational time of each algorithm is about 12 hours.

As can be seen from Fig. 12, the convergence of the PSO-IW algorithm is better than the GA. Although the GA can also gain the optimal results, its optimization performance is slightly less than the PSO-IW. Furthermore, other solution methods can also be used to solve this allocation model, such as the artificial bee colony (ABC) algorithm [43] and other improved GA and PSO algorithms.

One disadvantage of these two solution methods is that they need too much computation time because the established allocation model considered a wide variety of power fluctuation scenarios of PV. Nevertheless, this model also optimized the output power of the HESS, while allocating the HESS capacities. Fortunately, the allocation problem is an off-line optimization rather than a real-time (online) control. The allocation problem needs to consider numerous influencing factors, thus it is acceptable to spend much time on it.

4) OTHER FACTORS

Other parameters, such as the costs of batteries and supercapacitors, the unit price of solar energy, and the battery life will also affect the optimal capacities of the HESS and the revenue of the PV and HESS systems. Therefore, numerous simulations were carried out to investigate their impacts on optimization results. In conclusion, costs reduction in supercapacitors will increase the optimal capacities of the SCES and improve the system revenues. Furthermore, increasing the lifetime of batteries will correspondingly reduce the optimal energy capacities of the BES.

VI. CONCLUSIONS

In this work, a coordinated control strategy of the PV active power curtailment and the HESS is developed to mitigate the variations of PV power, ensuring the real-time active power variations at the PCC are less than ±10%/min of its rated capacity. Based on the proposed smoothing strategy, an

optimal sizing model of the HESS is established to optimize the energy and power capacities of the HESS, while maximizing the annual revenues of the PV and HESS systems. The main conclusions are as follows:

(1) The proposed allocation method has been proved to be effective in finding the optimal capacities of the HESS, which has fully considered the investment and operating costs of systems, lifetime aging costs of batteries, and the energy reduction in mitigating PV active power. Furthermore, it also considered a variety of scenarios of the PV power variations to guarantee the applicability and feasibility of the optimization results.

(2) This study has also shown that mitigating active power of PV can reduce the required capacity of supercapacitors, compared with the smoothing method of using the HESS alone. Also, the proposed smoothing strategy can also reduce the losses and costs of the HESS and improve the net revenues of the system.

(3) It has been found that the optimal energy and power capacities of the BES will increase and the optimal energy capacity of the SCES will decrease, as the allowable range of PV power variations becomes narrower.

A limitation of this study is that the calculation time of the proposed allocation model is relatively long because it optimizes the capacities and output power of the HESS at the same time. In addition, considering numerous possible scenarios of PV further increases its computational time. Therefore, further studies are required to reduce the number of typical scenarios of PV so that the calculation time could be reduced.

REFERENCES

[1] N. Tang, Y. Zhang, Y. Niu, and X. Du, "Solar energy curtailment in China: Status quo, reasons and solutions," *Renew. Sustain. Energy Rev.*, vol. 97, pp. 509–528, 2018.

[2] D. A. Elvira-Ortiz, D. Morinigo-Sotelo, O. Duque-Perez, A. Y. Jaen-Cuellar, R. A. Osornio-Rios, and R. D. J. Romero-Troncoso, "Methodology for flicker estimation and its correlation to environmental factors in photovoltaic generation," *IEEE Access*, vol. 6, pp. 24035–24047, 2018.

[3] K. W. Kow, Y. W. Wong, R. K. Rajkumar, and R. K. Rajkumar, "A review on performance of artificial intelligence and conventional method in mitigating PV grid-tied related power quality events," *Renew. Sustain. Energy Rev.*, vol. 56, pp. 334–346, Apr. 2016.

[4] P. Li, C. Zhang, X. Fu, G. Song, C. Wang, and J. Wu, "Determination of local voltage control strategy of distributed generators in active distribution networks based on Kriging metamodel," *IEEE Access*, vol. 7, pp. 34438–34450, 2019.

[5] J. Marcos, I. de la Parra, M. García, and L. Marroyo, "Control strategies to smooth short-term power fluctuations in large photovoltaic plants using battery storage systems," *Energies*, vol. 7, no. 10, pp. 6593–6619, 2014.

[6] X. Li, L. Yao, and D. Hui, "Optimal control and management of a large-scale battery energy storage system to mitigate fluctuation and intermittence of renewable generations," *J. Mod. Power Syst. Clean Energy*, vol. 4, no. 4, pp. 593–603, Oct. 2016.

[7] W. A. Omran, M. Kazerani, and M. M. A. Salama, "Investigation of methods for reduction of power fluctuations generated from large grid-connected photovoltaic systems," *IEEE Trans. Energy Convers.*, vol. 26, no. 1, pp. 318–327, Mar. 2011.

[8] X. Li, D. Hui, and X. Lai, "Battery energy storage station (BESS)-based smoothing control of photovoltaic (PV) and wind power generation fluctuations," *IEEE Trans. Sustain. Energy*, vol. 4, no. 2, pp. 464–473, Apr. 2013.

[9] M. Anvari, B. Werther, G. Lohmann, M. Wächter, J. Peinke, and H. P. Beck, "Suppressing power output fluctuations of photovoltaic power plants," *Sol. Energy*, vol. 157, pp. 735–743, Nov. 2017.

[10] I. de la Parra, J. Marcos, M. García, and L. Marroyo, "Improvement of a control strategy for PV power ramp-rate limitation using the inverters: Reduction of the associated energy losses," *Sol. Energy*, vol. 127, pp. 262–268, Apr. 2016.

[11] S. Sukumar, H. Mokhlis, S. Mekhilef, M. Karimi, and S. Raza, "Ramp-rate control approach based on dynamic smoothing parameter to mitigate solar PV output fluctuations," *Int. J. Elect. Power Energy Syst.*, vol. 96, pp. 296–305, 2018.

[12] I. de la Parra, J. Marcos, M. García, and L. Marroyo, "Control strategies to use the minimum energy storage requirement for PV power ramp-rate control," *Sol. Energy*, vol. 111, pp. 332–343, Jan. 2015.

[13] B. Zakeri and S. Syri, "Electrical energy storage systems: A comparative life cycle cost analysis," *Renew. Sustain. Energy Rev.*, vol. 42, pp. 569–596, Feb. 2015.

[14] C. Zhang, Y.-L. Wei, P.-F. Cao, and M.-C. Lin, "Energy storage system: Current studies on batteries and power condition system," *Renew. Sustain. Energy Rev.*, vol. 82, pp. 3091–3106, Feb. 2018.

[15] A. Makibar, L. Narvarte, and E. Lorenzo, "On the relation between battery size and PV power ramp rate limitation," *Sol. Energy*, vol. 142, pp. 182–193, Jan. 2017.

[16] A. S. Jacob, R. Banerjee, and P. C. Ghosh, "Sizing of hybrid energy storage system for a PV based microgrid through design space approach," *Appl. Energy*, vol. 212, pp. 640–653, Feb. 2018.

[17] X. Feng, J. Gu, and X. Guan, "Optimal allocation of hybrid energy storage for microgrids based on multi-attribute utility theory," *J. Mod. Power Syst. Clean Energy*, vol. 6, no. 1, pp. 107–117, 2017.

[18] C. K. Das, O. Bass, G. Kothapalli, T. S. Mahmoud, and D. Habibi, "Overview of energy storage systems in distribution networks: Placement, sizing, operation, and power quality," *Renew. Sustain. Energy Rev.*, vol. 91, pp. 1205–1230, Aug. 2018.

[19] M. Bucciarelli, S. Paoletti, and A. Vicino, "Optimal sizing of energy storage systems under uncertain demand and generation," *Appl. Energy*, vol. 225, pp. 611–621, Sep. 2018.

[20] Z. Hua, C. Ma, J. Lian, X. Pang, and W. Yang, "Optimal capacity allocation of multiple solar trackers and storage capacity for utility-scale photovoltaic plants considering output characteristics and complementary demand," *Appl. Energy*, vol. 238, pp. 721–733, May 2019.

[21] M. Cao, Q. Xu, J. Cai, and B. Yang, "Optimal sizing strategy for energy storage system considering correlated forecast uncertainties of dispatchable resources," *Int. J. Elect. Power Energy Syst.*, vol. 108, pp. 336–346, Jun. 2019.

[22] P. Zhao, J. Wang, and Y. Dai, "Capacity allocation of a hybrid energy storage system for power system peak shaving at high wind power penetration level," *Renew. Energy*, vol. 75, pp. 541–549, Mar. 2015.

[23] D. Álvaro, R. Arranz, and J. A. Aguado, "Sizing and operation of hybrid energy storage systems to perform ramp-rate control in PV power plants," *Int. J. Elect. Power Energy Syst.*, vol. 107, pp. 589–596, May 2019.

[24] N. Yan, B. Zhang, W. Li, and S. Ma, "Hybrid energy storage capacity allocation method for active distribution network considering demand side response," *IEEE Trans. Appl. Supercond.*, vol. 29, no. 2, Mar. 2019, Art. no. 5700204.

[25] W. Ma, W. Wang, X. Wu, R. Hu, F. Tang, and W. Zhang, "Control strategy of a hybrid energy storage system to smooth photovoltaic power fluctuations considering photovoltaic output power curtailment," *Sustainability*, vol. 11, no. 5, p. 1324, 2019.

[26] W. Jiang, L. Zhang, H. Zhao, R. Hu, and H. Huang, "Research on power sharing strategy of hybrid energy storage system in photovoltaic power station based on multi-objective optimisation," *IET Renew. Power Gener.*, vol. 10, no. 5, pp. 575–583, 2016.

[27] A. Evans, V. Strezov, and T. J. Evans, "Assessment of utility energy storage options for increased renewable energy penetration," *Renew. Sustain. Energy Rev.*, vol. 16, no. 6, pp. 4141–4147, 2012.

[28] L. Wang, S. Sharkh, A. Chipperfield, and A. Cruden, "Dispatch of vehicle-to-grid battery storage using an analytic hierarchy process," *IEEE Trans. Veh. Technol.*, vol. 66, no. 4, pp. 2952–2965, Jul. 2017.

[29] Y. Zhang, P. E. Campana, A. Lundblad, and J. Yan, "Comparative study of hydrogen storage and battery storage in grid connected photovoltaic system: Storage sizing and rule-based operation," *Appl. Energy*, vol. 201, pp. 397–411, Sep. 2017.

[30] B. Xu, A. Oudalov, A. Ulbig, G. Andersson, and D. S. Kirschen, "Modeling of lithium-ion battery degradation for cell life assessment," *IEEE Trans. Smart Grid*, vol. 9, no. 2, pp. 1131–1140, Mar. 2018.
[31] G. He, Q. Chen, C. Kang, Q. Xia, and K. Poolla, "Cooperation of wind power and battery storage to provide frequency regulation in power markets," *IEEE Trans. Power Syst.*, vol. 32, no. 5, pp. 3559–3568, Dec. 2017.
[32] C. A. Correa-Florez, A. Gerossier, A. Michiorri, and G. Kariniotakis, "Stochastic operation of home energy management systems including battery cycling," *Appl. Energy*, vol. 225, pp. 1205–1218, Sep. 2018.
[33] M. Musallam and C. M. Johnson, "An efficient implementation of the rainflow counting algorithm for life consumption estimation," *IEEE Trans. Rel.*, vol. 61, no. 4, pp. 978–986, Dec. 2012.
[34] C. Du, Z. Yin, Y. Zhang, J. Liu, X. Sun, and Y. Zhong, "Research on active disturbance rejection control with parameter autotune mechanism for induction motors based on adaptive particle swarm optimization algorithm with dynamic inertia weight," *IEEE Trans. Power Electron.*, vol. 34, no. 3, pp. 2841–2855, Mar. 2019.
[35] P. Hou, W. Hu, B. Zhang, M. Soltani, C. Chen, and Z. Chen, "Optimised power dispatch strategy for offshore wind farms," *IET Renew. Power Gener.*, vol. 10, no. 3, pp. 399–409, 2016.
[36] V. Sarfi and H. Livani, "An economic-reliability security-constrained optimal dispatch for microgrids," *IEEE Trans. Power Syst.*, vol. 33, no. 6, pp. 6777–6786, Nov. 2018.
[37] C. S. Lai, Y. Jia, M. D. McCulloch, and Z. Xu, "Daily clearness index profiles cluster analysis for photovoltaic system," *IEEE Trans. Ind. Informat.*, vol. 13, no. 5, pp. 2322–2332, Oct. 2017.
[38] IRENA. (2018). *Renewable Power Generation Costs in 2017*. [Online]. Available: http://www.irena.org/publications/2018/Jan/Renewable-power-generation-costs-in-2017
[39] IRENA. (2017). *Electricity Storage and Renewables: Costs and Markets to 2030*. [Online]. Available: https://www.irena.org/public-ations/2017/Oct/Electricity-storage-and-renewables-costs-and-markets
[40] IRENA. (2016). *The Power to Change: Solar and Wind Cost Reduction Potential to 2025*. [Online]. Available: http://www.irena.org/publications%20/2016/Jun/The-Power-to-Change-Solar-and-Wind-Cost-Reduction-Potential-to-2025
[41] U.S. Energy Information Administration. (2018). *Electric Power Monthly*. [Online]. Available: https://www.eia.gov/electricity/monthly/index.php
[42] A. Arias-Rosales and R. Mejía-Gutiérrez, "Optimization of V-Trough photovoltaic concentrators through genetic algorithms with heuristics based on Weibull distributions," *Appl. Energy*, vol. 212, pp. 122–140, Feb. 2018.
[43] K. Liu, C. Wang, and S. Liu, "Artificial bee colony algorithm combined with previous successful search experience," *IEEE Access*, vol. 7, pp. 34318–34332, 2019.

WEI MA (S'19) received the B.Eng. and M.E. degrees in electrical engineering from Beijing Jiaotong University, Beijing, China, in 2014 and 2016, respectively, where he is currently pursuing the Ph.D. degree. His current research interests include photovoltaic (PV) systems, energy storage systems, and the optimization of active distribution networks.

WEI WANG received the B.S. and M.S. degrees in electrical engineering from Northeast Dianli University, Jilin, China, in 1982 and 1988, respectively. He is currently a Professor with the School of Electrical Engineering, Beijing Jiaotong University, China. He was a Leader for over 30 applied projects and has authored over 60 research papers in journals and conferences. His research interests include power systems and power electronics. His current research interests include power system analysis and control, and active distribution system technology.

XUEZHI WU received the Ph.D. degree in power electronics and electric drives from Tsinghua University, Beijing, China, in 2002. He is currently an Associate Professor with the Department of Electrical Engineering, Beijing Jiaotong University, Beijing. His current research interests include microgrids, wind power generation systems, power converters for renewable generation systems, power quality, and motor control.

RUONAN HU (S'19) received the B.Eng. degree in electrical engineering from Beijing Jiaotong University, Beijing, China, in 2016, where she is currently pursuing the Ph.D. degree. Her current research interests include the operation and control of soft open points in active distribution networks, the application of power electronic devices in the power systems, and the optimization of active distribution networks.

FEN TANG received the B.S. degree in electrical engineering and the Ph.D. degree in power electronics and electric drives from Beijing Jiaotong University, Beijing, China, in 2006 and 2013, respectively, where she has been a Lecturer, since 2015. She was a Guest Postdoctoral Researcher with the Department of Energy Technology, Aalborg University, Aalborg, Denmark, from 2013 to 2014. Her current research interests include microgrids, wind power generation systems, power converters for renewable generation systems, power quality, and motor control.

WEIGE ZHANG received the M.S. and Ph.D. degrees in electrical engineering from Beijing Jiaotong University, Beijing, China, in 1997 and 2013, respectively, where he is currently a Professor with the School of Electrical Engineering. His research interests include battery pack application technology, power electronics, and intelligent distribution systems.

XIAOYAN HAN was born in 1965. He received the Ph.D. degree in electrical engineering from Zhejiang University, Hangzhou, China, in 1995. He is currently the Deputy Chief Engineer with State Grid Sichuan Electric Power Company, Chengdu, China. His main research interest includes power system operation and control.

LIJIE DING was born in 1981. He received the Ph.D. degree in electrical engineering from Zhejiang University, Hangzhou, China, in 2008. He is currently the Chief Engineer with the State Grid Sichuan Electric Power Research Institute, Chengdu, China. His main research interest includes power system transient stability analysis and control.